POLAR 2018

Where the Poles come together

Abstract Proceedings

Open Science Conference
19 – 23 June 2018
Davos, Switzerland

IASC

A SCAR and IASC Event

SCAR

A-938-0060-02475

FACTORS CONTROLLING WATER MASS VARIATIONS OVER THE CHUKCHI BORDERLAND, ARCTIC

K.-H. Cho[1] · Y.-S. Choi[2] · E. Yoshizawa[1] · S. Kim[1,2] · T. Park[1] · S.-H. Kang[1]

[1]Korea Polar Research Institute, Republic of Korea
[2]Inha University, Republic of Korea

ABSTRACT: *We have carried out hydrographic surveys since 2010 to monitor the Pacific-origin waters over the Chukchi Borderland (CBL) in the western Arctic Ocean. Based on CTD/XCTD data analysis, the heat content from the Pacific Summer Water (PSW) is highly correlated with sea ice extent reduction over the region. Yearlong mooring and numerical simulation data are analyzed to verify what factors lead the PSW variation. We found two factors controlling the variation of PSW over the region: variation of summer waters incoming through the Bering Strait (BS) and variation of local winds over the East Siberian Sea (ESS) shelf. Temporal variation of PSW temperature over CBL is in-phase with that of the Alaskan Coastal Water (ACW) temperature even if there is a time lag. Relatively cold water over the ESS shelf is transported to the CBL by local winds and subducted into the PSW layer by the thermohaline intrusion.*

1 INTRODUCTION

◆ Background

1) Arctic warming and sea ice reduction trends

- Rapid increase of annual mean land surface air temperature in the Arctic since 2000 (Fig.1a)
- Sea ice extent in September: 13.2 %/decade reduction relative to 1981-2010 mean (Fig.1b)
- SIE shows interannual variation since 2007 (Fig.1b)

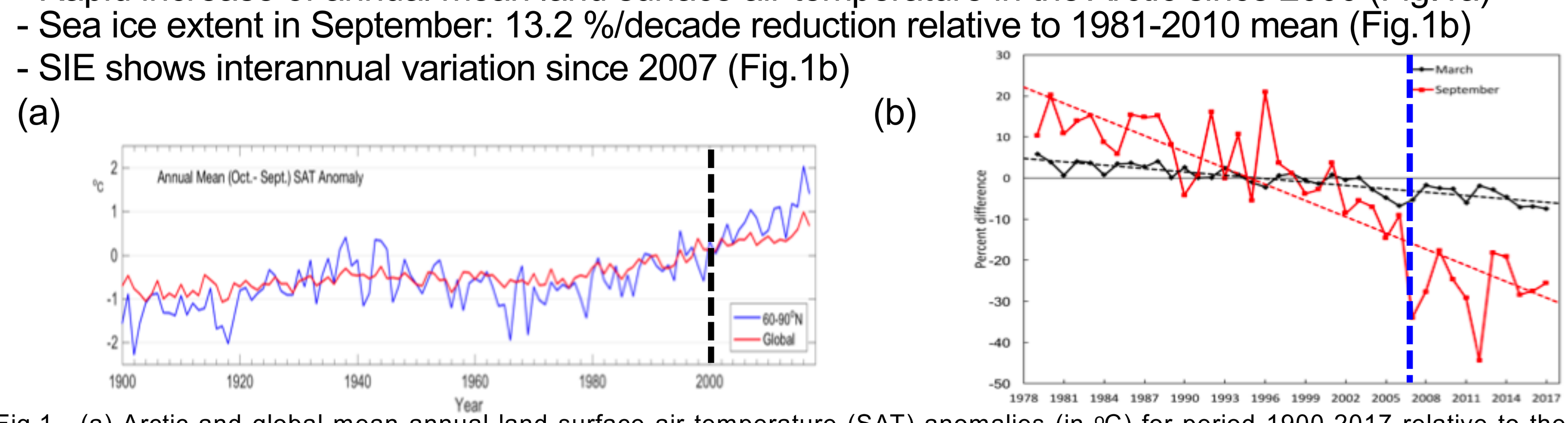

Fig.1. (a) Arctic and global mean annual land surface air temperature (SAT) anomalies (in °C) for period 1900-2017 relative to the 1981-2010 mean value (*Overland et al., 2017*) and (c) time series of ice extent anomalies (in %) in March and September relative to the mean values for the period 1981-2010 (*Perovich et al., 2017*).

2) Sea surface temperature (SST) in the western Arctic Ocean

- Surface heat radiation increase due to ice reduction; increase of Pacific-origin water's temperature -> SST increase (Fig.2a)
- In the Chukchi Sea, SST increases by 0.07 ℃ / year (Fig. 2b)

3) Variation of sea ice extent on September in wAO

- Similar pattern to that in the East Siberian Sea since 2007
- Relatively high SIE on September: Years 2009, 2013-14, and 2016-17

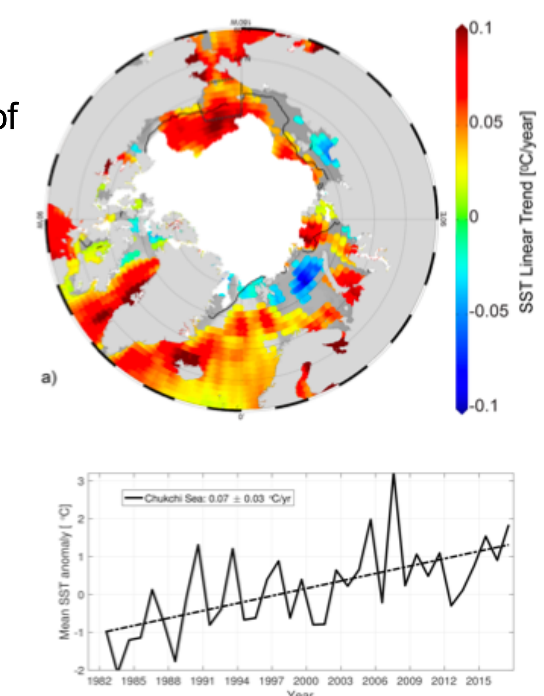

Fig.2. (a) Linear SST trend (°C yr⁻¹) for August of each year from 1982-2017 and (b) Area-averaged SST anomalies (oC) for August of each year relative to the 1982-2010 August mean for the Chukchi Sea region shown by the dotted lines in (a) (*Timmermans et al., 2017*).

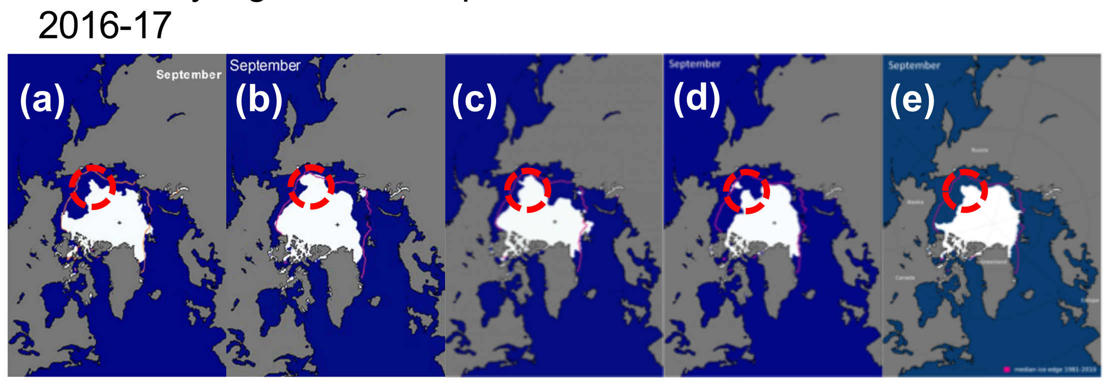

Fig.3. Distribution of sea ice in September of (a) 2009, (b) 2013, (c) 2014, (d) 2016 and (e) 2017. Red dotted circles indicate the East Siberian Sea region (*Perovich et al., 2017*).

◆ Research Objective

- This study aims to understand the factors which affect the variations of the water masses over the Chukchi Borderland, western Arctic Ocean using the observation data and model reanalysis data.

2 DATA

◆ KOPRI Arctic Expeditions (2010~2017)

1) CTD/XCTD data

a) Hydrographic surveys using IBRV ARAON (Fig.4)
 : CTD, lowered ADCP, XCTD, ocean moorings, etc.

b) CTD data calibration

- C and T - Pre-/post-cruise lab calibration
- Sea water sampling: AUTOSAL salinometer

c) Potential T and σ

- TEOS-10 toolbox (*McDougall and Barker, 2011*)
- Accuracy: ±0.0003 S/m (C), ±0.001 ℃ (T)

d) XCTD data calibration: 3 XCTD probes dropped at 3 CTD stations and calibrated

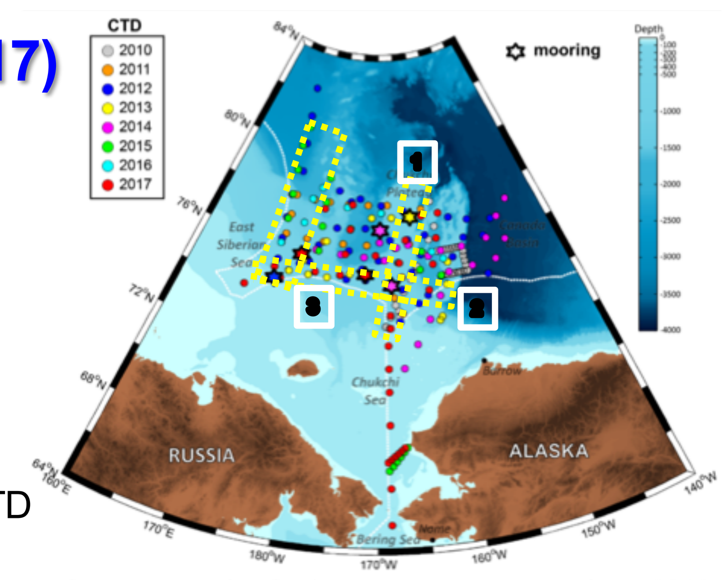

Fig.4. Station map for CTD and ocean mooring from 2010 to 2017. Colored dashed boxes represent 3 transects.

2) Ocean Mooring Systems

a) Five mooring systems were recovered from the ice breaker R/V ARAON (Figs. 4)
- 2012 to 2013: ESS-12 and ESC-12
- 2013 to 2015: CP13
- 2014 to 2015: CP14, GAM2 (ADCPs, microCATs, temperature loggers, MMP-type CTD, etc.)

b) Items measured from the mooring systems
- Temperature, salinity, water velocity, ice speed, pressure, etc.

◆ Collection of other datasets

1) Sea ice data

a) Sea ice draft for first year ice (FYI): used polarized brightness temperature, AMSR2 level3(L3) products provided by the JAXA (https://gcom-w1.jaxa.jp) (Fig.5)
b) Sea ice concentration (SIC): AMSR2 data from Univ. of Bremen (http://www.iup.unibremen.de:8084/amsr2data/)
c) Sea ice velocity (SIV): calculated by the particle image velocimetry method applied for AMSR2 daily brightness temperature images (*Kamoshida and Shimada, 2010*)

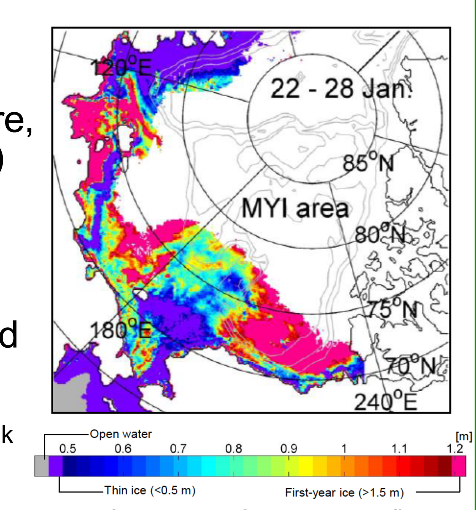

Fig.5. Estimated FYI draft for the 4th week January 2017 (*Yoshizawa et al., in review*)

2) Re-analysis data

a) Atmospheric: ECMWF ERA-interim monthly data (http://apps.ecmwf.int/datasets/interim-full-moda/)
b) Oceanic: PIOMAS data
(*Zhang and Rothrock, 2003*; http://psc.apl.uw.edu/research/projects/arctic-sea-ice-volume-anomaly/data/)
c) Others : - Dynamic ocean topography (DOT) for the period 2003-2014 (*Armitage et al., 2016;* http://www.cpom.ucl.ac.uk/):
- Envisat data for 2003-2011 and CryoSat-2 data for 2012-2014; SSH estimates are referenced to the GOCO03s combined satellite-only geoid model (http://www.goco.eu/).

3 RESULTS

◆ Water Mass Property

1) T-S diagram analysis

a) Some water masses are distinctly distributed in study area: Pacific Summer Water (PSW), Pacific Winter Water (PWW), and Atlantic Water (AW) (Fig.6)
b) In 2017 summer,
- Cold water mass which has low θ ($\sigma_\theta \approx$ 25.5~26 kg/m^3, S~32 psu)
 >> presumed to be formed on the East Siberian Shelf during winter
- Relatively cold water mass between PWW and AW ($\sigma_\theta \approx$ 27.5~27.7 kg/m^3, S~34.5 psu) >> extended from the eastern Arctic

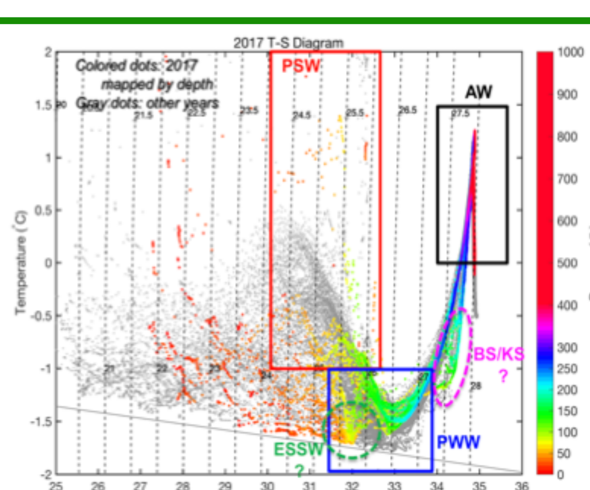

Fig.6. T-S diagram from 2017 CTD data (colored dots). Colored solid boxes represent predominant water masses found. Gray dots represent other years

2) Horizontal distribution of PSW

- Maximum potential temperature within PSW (Fig.7)
- Increased in 2012-2013; decreased in 2014, 2016

3) Horizontal distribution of PWW

- Minimum potential temperature within PSW (Fig.8)
- Increased in 2012-2013; decreased in 2014, 2016

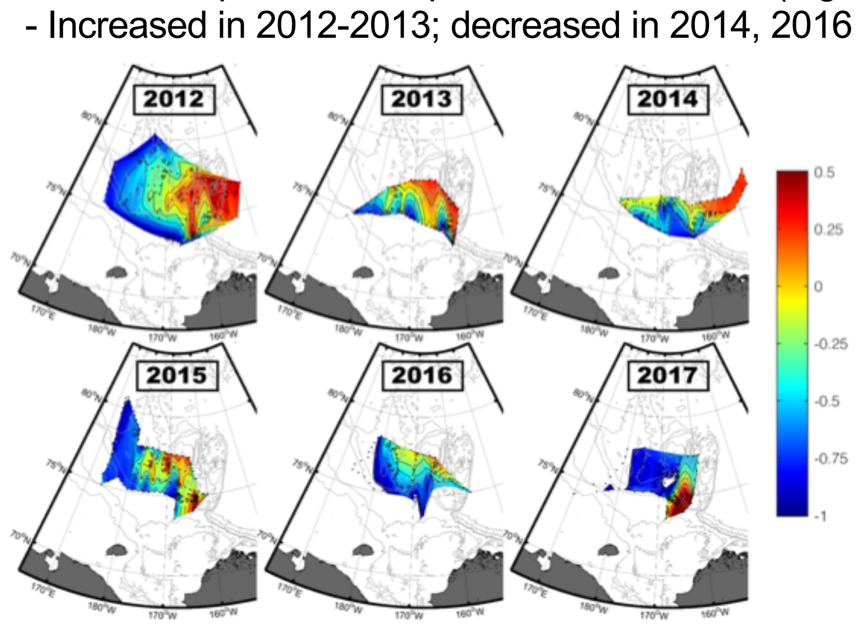

Fig.7. Horizontal distribution of PSW maximum θ from 2012 to 2017.

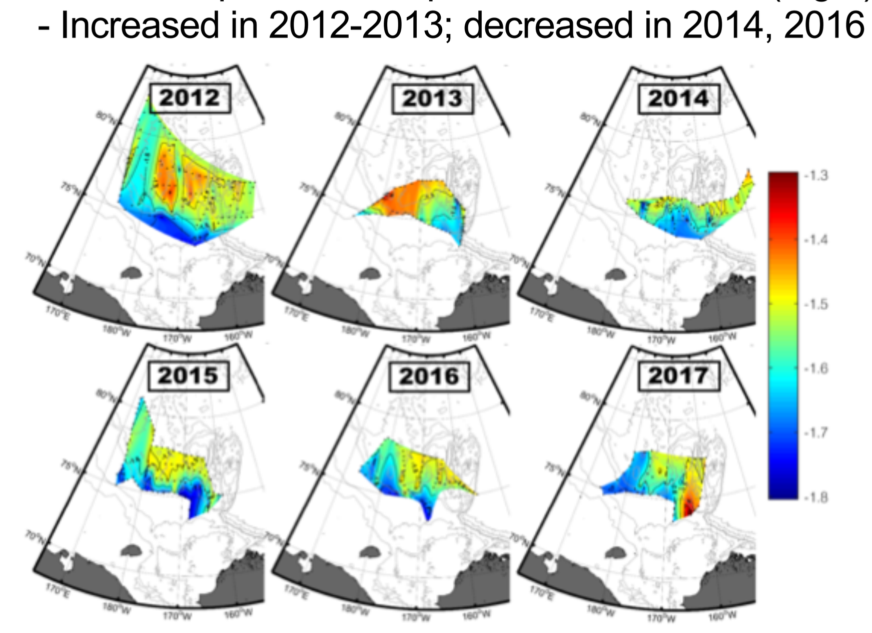

Fig.8. Horizontal distribution of PWW maximum θ from 2012 to 2017.

◆ Correlation Analysis I

Correlations between variables

a) Sea ice extent (SIE) anomaly vs. PSW θ anomaly (Fig.9a)
b) Sea ice extent (SIE) anomaly vs. mixed water S anomaly (Fig.9b)
c) Cross-shelf Wind anomaly vs. PSW θ anomaly (Fig.9c)

* Variables averaged over:
- Ocean: 74°~78°N, 170°W~160°W
- Sea ice : 70°~85°N, 180°W~165°W
- Atmosphere : 72°~82°N, 150°E~150°W

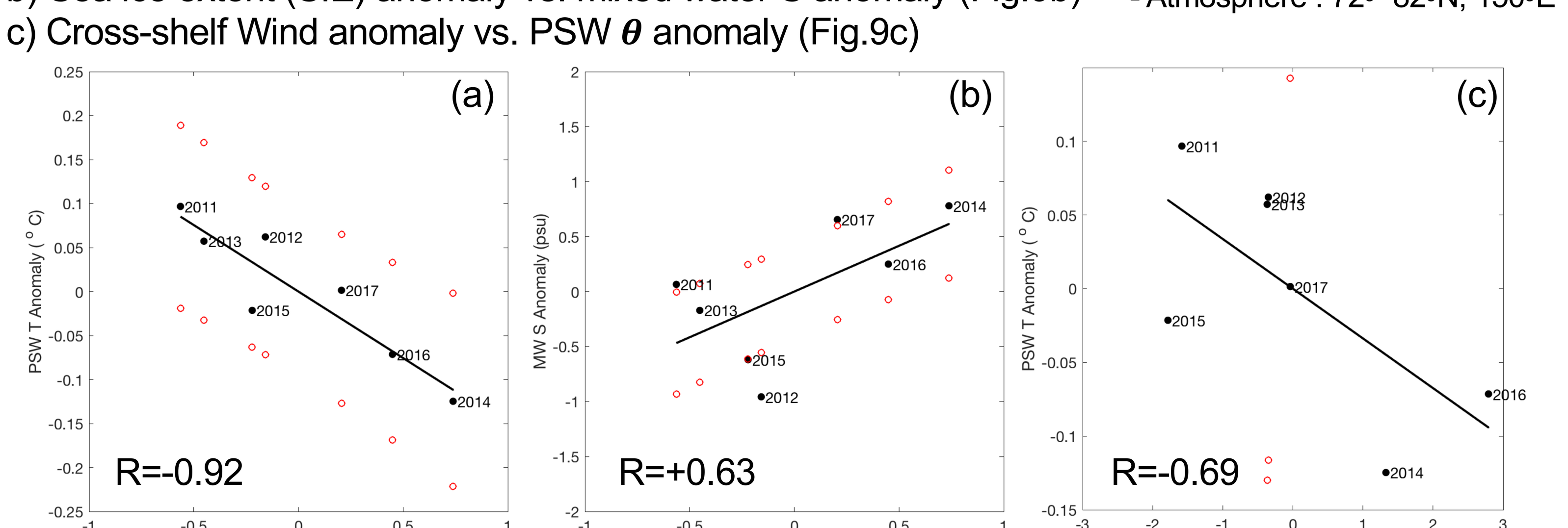

Fig.9. Correlations between variables of water masses, sea-ice extent, and atmosphere in summer: a) SIE anomaly vs. PSW θ anomaly, b) SIE anomaly vs. MW S anomaly, and c) cross-shelf wind anomaly vs. PSW θ anomaly.

◆ Correlation Analysis II

Correlations between oceanic variables from reanalysis dataset

a) PSW intensified from March at GAM2 site (Fig.10)
b) Lag correlation between T over Bering Strait and T over CAP (Fig.11) [used PIOMAS]

>> This implies that Pacific-origin water via Bering Strait would reach to CAP after 4~6 months.

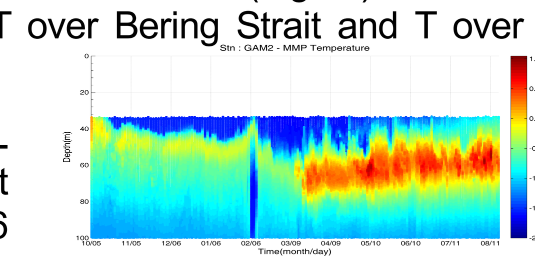

Fig.10. Temporal plot of water temperature observed at GAM2 mooring station.

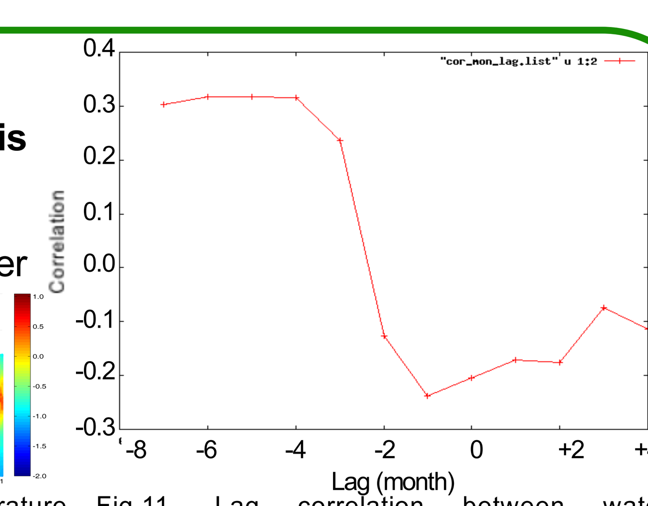

Fig.11. Lag correlation between water temperatures of BS and CAP (March).

◆ Thermohaline Intrusion (ongoing)

Intrusion of cold water masses

- As described in water mass property section, two cold waters intrusion

a) Cold water mass which has low θ ($\sigma_\theta \approx$ 25.5~26 kg/m^3, S~32 psu)
b) Relatively cold water mass between PWW and AW ($\sigma_\theta \approx$ 27.5~27.7 kg/m^3, S~34.5 psu)

- This will be further analyzed for the future study.

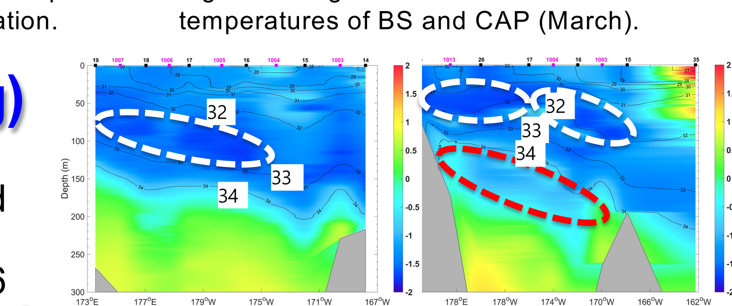

Fig.12. Vertical profiles of S, T at Transects 2 depicted in Fig.4: 2016 (left) and 2017 (right)

◆ Sea Ice Analysis (ongoing)

Sea ice draft (SID) distribution

- Distribution of SIC on summer appears to be influenced by two ice factors: 1) Pattern of sea ice formation during previous winter and 2) Convergence of sea ice motion (Fig.13)
- This will be further analyzed for the future study.

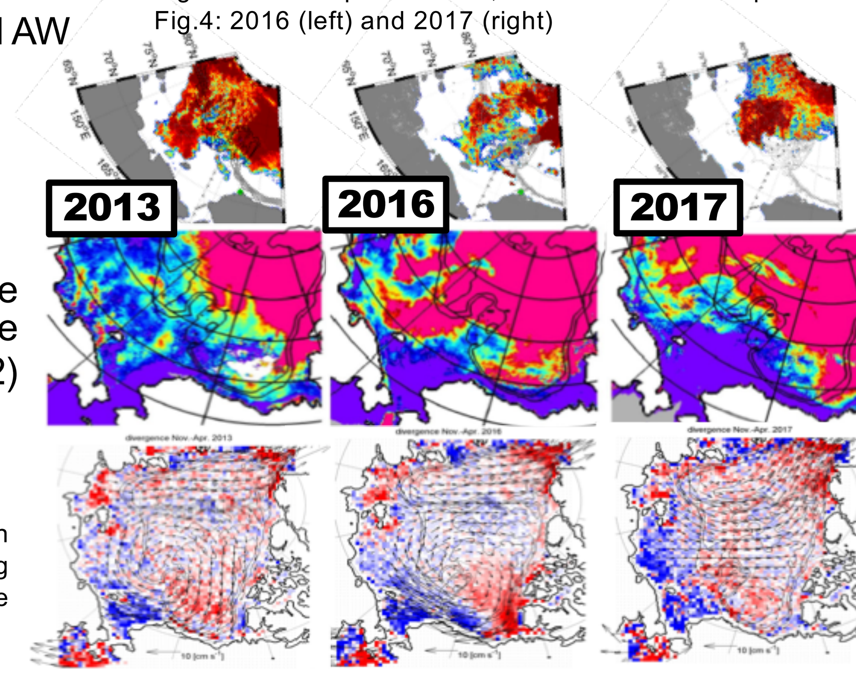

Fig.13. Sea ice concentration in August (upper), sea ice draft in January (middle), and divergence of ice motion vectors during winters (lower) of 2013 (left), 2016 (center), and 2017 (right). Blue color stands for convergence.

4 SUMMARY

* Please contact Kyoung-Ho Cho at kcho@kopri.re.kr if you have any questions.

- ◆ We analyzed ocean survey data, sea ice data, and numerical re-analysis data to investigate recent behaviors of the Pacific-origin waters around the Chukchi Borderland (CBL).
- ◆ In August, anomaly of sea ice extent (SIE) has a negative correlation with that of PSW temperature whereas it has a positive correlation with that of MW salinity. This implies that inter-annual variation of PSW temperature plays an important role on the trend of sea ice melting and consequent ice melting has an influence on salinity reduction in the surface melt water layer. Anomaly of PSW T is correlated with anomaly of cross-shelf wind, that is, southerly/southwesterly winds tends to restrict westward flow which drives PSW extending to the west.
- ◆ Based on analysis of PIOMAS dataset, PSW T on CAP during Feb to April appears to have a good correlation with that on Bering Strait during August. This implies that it takes 4~6 months that Pacific-origin water via Bering Strait reaches the Chukchi Abyssal Plain area.

Acknowledgement

This research was a part of the project titled `Korea-Arctic Ocean Observing System(K-AOOS, KOPRI, 20160245)` funded by the Ministry of Oceans and Fisheries, Korea.